CLINICAL TRIAL

JBMR®

Skeletal Changes After Hematopoietic Stem Cell Transplantation in Osteopetrosis

Galina Shapiro,[1] Jorge Fishleder,[2] Polina Stepensky,[3] Naum Simanovsky,[2] Vladimir Goldman,[2] and Ron Lamdan[4]

[1]Medical Corps, Israel Defense Forces, Ramat Gan, Israel
[2]Pediatric Orthopedics Unit, Department of Orthopedic Surgery, Hadassah-Hebrew University Medical Center, Jerusalem, Israel
[3]Department of Bone Marrow Transplantation and Cancer Immunotherapy, Hadassah-Hebrew University Medical Center, Jerusalem, Israel
[4]Pediatric Orthopedics Unit, Assuta Ashdod Medical Center, Ashdod, Israel

ABSTRACT

Osteopetrosis is a rare skeletal dysplasia resulting from an osteoclast defect leading to increased bone mass and density. Hematopoietic stem cell transplantation can rescue the disease phenotype and prevent complications. However, little is known about the skeletal changes hematopoietic stem cell transplantation induces in patients with this disease. The purpose of this study was to describe the skeletal changes after hematopoietic stem cell transplantation in a retrospective cohort of patients diagnosed with osteopetrosis in one medical center over 13 years. For this purpose, all available epidemiological, hematological, biochemical, and radiographic data were collected and quantitatively analyzed. We found a significant early change in bone metabolism markers coinciding with hematopoietic recovery after stem cell transplantation. Hematopoietic stem cell transplantation induced a later significant improvement in both skeletal mineral distribution and morphology but did not lead to complete radiological normalization. Presumably, changes in bone metabolism, skeletal mineral distribution, and morphology were the result of renewed osteoclast function enabling bone remodeling. We propose that biochemical bone metabolism markers and radiological indices be routinely used to evaluate response to hematopoietic stem cell transplantation in patients with osteopetrosis. © 2020 American Society for Bone and Mineral Research.

KEY WORDS: BIOCHEMICAL MARKERS OF BONE TURNOVER; CLINICAL TRIALS; OSTEOPETROSIS; OSTEOCLASTS; RADIOLOGY

Introduction

Osteopetrosis (OP) refers to a heterogeneous group of rare inherited skeletal dysplasias, characterized by quantitative or qualitative osteoclast defects that lead to increased bone mass and density.[1] Multiple genetic defects underlie both the adult-onset autosomal dominant OP (ADO) and the more severe, and often fatal if untreated, autosomal recessive OP (ARO).[2] Most of these mutations are osteoclast-specific defects in late endosomal trafficking, preventing osteoclast ruffled border formation. The disease phenotype can be rescued by providing a healthy osteoclast population via hematopoietic stem cell transplantation (HSCT).[3] Without HSCT, secondary complications may develop, including bone marrow failure,[4] cranial nerve dysfunction,[5,6] and pathological fractures.[7]

OP is associated with a multitude of skeletal abnormalities. Pathological fractures and growth retardation with short stature are common. Cranial pathological features include macrocephaly, frontal bossing, and micrognathia. In long bones, characteristic radiographic findings include a "bone-within-bone" appearance, transverse lucent metaphyseal bands, longitudinal diaphyseal striations, and Erlenmeyer flask deformities.[8,9] In the spine, vertebral endplate sclerosis results in a "sandwich" or "rugger-jersey" appearance. A unique radiographic appearance was described for a subgroup of patients with *TCIRG1* mutations who suffered from OP and rickets. Called osteopetrorickets, the condition has been found to be caused by reduced gastrointestinal Ca2+ uptake and the consequent inability to fully mineralize newly formed osteoid.[10,11]

In most patients, OP can be diagnosed by combining radiographic findings with genetic analysis of key genes.[3,12] The latter is also valuable in guiding treatment, as in the case of *RANKL*-related mutations, which are a contraindication for HSCT.[6,13] Preferably, HSCT is done in children younger than 1 year of age, from related HLA-matched donors.[14] Recent advances in HSCT have greatly improved life expectancy and quality of life of ARO patients, with 10-year survival rate getting as high as 62%, achieving acceptable social function.[14]

OP patients who have undergone HSCT are followed closely to establish engraftment and rule out complications including graft-versus-host disease (GVHD), veno-occlusive disease of the liver, and graft failure. Hypercalcemia may be found early on, indicating bone remodeling by functional osteoclasts

Received in original form October 15, 2019; revised form March 30, 2020; accepted April 16, 2020; Accepted manuscript online April 24, 2020.
Address correspondence to: Ron Lamdan, MD, Ha-Refu'a Street 7, Ashdod 7747629, Israel. E-mail: ronortho@gmail.com
Journal of Bone and Mineral Research, Vol. 35, No. 9, September 2020, pp 1645–1651.
DOI: 10.1002/jbmr.4037

differentiated from transplanted progenitors.[15–17] However, little is known about the remodeling process and consequent skeletal changes, despite their great impact on patient quality of life. Radiological improvement after HSCT up to a year after the transplantation has been studied only in case reports and small series with no quantitative outcomes.[18–20] These studies used qualitative X-ray evaluations to conclude that HSCT results in almost complete resolution of skeletal abnormalities. A more comprehensive characterization of the skeletal changes in OP patients after HSCT could be useful in optimizing treatment, with the ultimate goal of curing the skeletal abnormalities associated with OP.

We hypothesized that HSCT in OP patients induces bone remodeling that improves but does not entirely cure the skeletal abnormalities associated with OP. To evaluate this hypothesis, we examined a cohort of HSCT-treated OP patients of the greatest size and longest follow-up time to date. We investigated hematopoietic and bone remodeling recovery after HSCT to evaluate whether HSCT induced a measurable remodeling effect. Then we developed novel quantitative indices of bone mineral distribution and morphology. These indices were used to compare the skeletal features of HSCT-treated OP patients with healthy age-matched controls to assess whether HSCT completely cured the disease phenotype. To the best of our knowledge, this is the first study to research the skeletal changes after HSCT in OP patients by quantitatively analyzing biochemical and radiological changes in a large cohort over a long follow-up period.

Materials and Methods

Patient and transplant characteristics

Radiographs of 35 patients taken between May 2003 and September 2016 were included in this retrospective study. A clinical diagnosis of OP has been confirmed by radiographic findings and, from 2008, by genetic analysis. All guardians signed informed consent before the HSCT. The study was approved by the Institutional Review Board.

The study population consisted of 35 children diagnosed with OP. Patient, disease, and transplant characteristics are presented in Table 1. {TBL 1} Patient sex, parent consanguinity, and a genetic diagnosis when available (mutations in TCIRG1, SNX10, CLCN7, OSTM1, or RANK genes) were collected to describe the patient population. The HSCTs (n = 36) are described in terms of the patient's age at the time of the HSCT, donor HLA-matching, and the conditioning regimen. Peripheral blood stem cells were mobilized and collected as previously published.[15]

GVHD prophylaxis and in vivo T-cell depletion

GVHD prophylaxis regimen and use of in vivo T-cell depletion in the patient group are described in Table 1. Patients received GVHD prophylaxis with either cyclosporine A only (n = 11, 3 mg/kg per day, intravenously as a single agent, starting on day −1), or in combination with mycophenolate mofetil (n = 8). Cyclosporine A administration in patients without signs of GVHD was continued for at least 3 months and was tapered thereafter. Acute and chronic GVHD were diagnosed using previously published criteria[21] and immediately treated with methylprednisolone (2 mg/kg) and combined modalities. Patients also received in vivo T-cell depletion in preparation for 31 HSCTs, using rabbit antithymocyte globulin or Campath-1H in one case.

Table 1 Patient and Transplant Characteristics

Patients	(n = 35)
Sex, n (%)	
Male	25 (71)
Female	10 (29)
Consanguineous parents, n (%)	17 (49)
Mutation, n (%)	
TCIRG1	20 (60)
SNX10	6 (18)
CLCN7	3 (9)
OSTM1	1 (3)
RANK	3 (9)
Age (years) at HSCT, median (range)	1.1 (0–13.4)
Donor match, n (%)	
Matched sibling donor	13 (36)
Matched family donor	5 (14)
Mismatched family donor	7 (19)
Matched unrelated donor	6 (17)
Mismatched unrelated donor	3 (8)
Conditioning regimen, n (%)	
Fludarabine-busulfan-melphalan	1 (3)
Fludarabine-busulfan	6 (17)
Fludarabine-busulfan-thiotepa	8 (22)
Fludarabine-treosulfan-thiotepa	18 (50)
GVHD prophylaxis, n (%)	
Cyclosporine A	27 (75)
Cyclosporine A–mycophenolate mofetil	9 (25)
In vivo T-cell depletion, n (%)	31 (86)
Age (years) at radiographic follow-up, n (%)	
<2	38 (40)
2–5	35 (37)
6–10	17 (18)
11–15	4 (4)
Follow-up (years), median (range)	4 (0–15)

HSCT = hematopoietic stem cell transplantation; GVHD = graft-versus-host disease.

Serotherapy was given for a total of 3 days, starting from 4 days before the HSCT, as a part of a conditioning regimen.

Supportive care and follow-up

All patients received trimethoprim-sulfamethoxazole for *Pneumocystis jirovecii* prophylaxis and acyclovir for Varicella zoster virus (VZV) prophylaxis for 6 months. Allopurinol was given to all patients for tumor-lysis syndrome prevention during conditioning. Patients were isolated in rooms equipped with high-efficiency particulate arrestance (HEPA) filters, and received a regular diet unless total parenteral nutrition was indicated. Blood product transfusions including red blood cells, platelets, and intravenous immunoglobulin (IVIG) were also administered as indicated.

Patients were monitored for post-HSCT complications including GVHD, viral reactivation, veno-occlusive disease, hypercalcemia, and pulmonary hypertension. Cytomegalovirus (CMV) PCR was performed weekly, and in a case of reactivation a preemptive antiviral treatment, including either ganciclovir, valganciclovir, or foscarnet, was started. Comprehensive metabolic panels were used to screen for electrolyte imbalances and especially hypercalcemia, which was initially treated with intravenous fluids and furosemide, whereas refractory cases required calcitonin and prednisolone.

Finally, the distribution of patient age during radiographic follow-up, based on radiographs available for densitometry analysis and follow-up length, were analyzed (Table 1). The latter was defined as the time between the first X-ray taken and the last follow-up visit.

Control group characteristics

Forty-six patients (28 males and 18 females, ages 0 to 15 years [median age 9 years]) evaluated at the Hadassah Hebrew University Medical Center from November 2006 to August 2016, for whom a normal anterior-posterior thigh X-ray was available were included as the control group. Radiographs were grouped into the following four groups based on the patient's age (years): 0–3 (n = 14), 4–7 (n = 8), 8–11 (n = 12), and 12–15 (n = 12).

Hematopoietic recovery

The number of days between HSCT and the first stable absolute neutrophil counts (ANC) above 0.5×10^9/L (Fig. 1*A*, {FIG1} normal laboratory values: 2–7.5×10^9/L) and platelet (PLT) counts above 20×10^9/L (Fig. 1*B*, normal laboratory values: 140–400×10^9/L) were used to study HSCT engraftment kinetics. Counts were deemed stable if they were above the cut-off for a minimum of 3 consecutive days. Data were available for 28 patients, and a paired t test was used to compare the number of days between HSCT and the first stable absolute neutrophil counts.

Bone metabolism analysis

Available serum calcium (Fig. 2*A*, {FIG2} normal laboratory values: 2.15–2.55 mmol/L, n = 30–32), phosphate (Fig. 2*B*, normal laboratory values: 0.8–1.4 mmol/L, n = 27–30), and alkaline phosphatase (Fig. 2*C*, ALP, normal laboratory values: 40–200 U/L, n = 28) measurements were compared for each patient on the day of their HSCT (denoted t0) and on the day of the maximal calcium measurement for each patient (denoted t1) using an unpaired t test. The number of days for each patient between HSCT and calcium peak was also recorded.

Orthopedic/radiological follow-up

All patients had supine radiographs of the lower extremities before HSCT as a baseline. Additional radiographs were obtained in 3- to 6-month intervals, in conjunction with routine clinical follow-up. All radiographs taken before the first radiological follow-up at 3 months post-HSCT were termed "early," whereas all radiographs taken after 3 months post-HSCT were termed "late." Radiographs were used to assess the morphological and cortex-to-medullary density changes after HSCT.

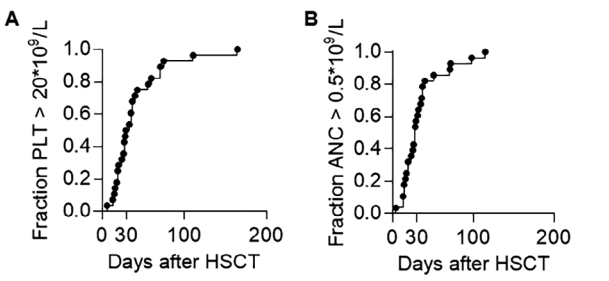

Fig 1 Hematopoietic recovery after HSCT. (*A*) Patients achieved absolute neutrophil counts (ANC) above 0.5×10^9/L in 4 to 115 days after HSCT with a median of 28 days. (*B*) Patients achieved platelet (PLT) counts above 20×10^9/L in 6 to 165 days after HSCT with a median of 31 days.

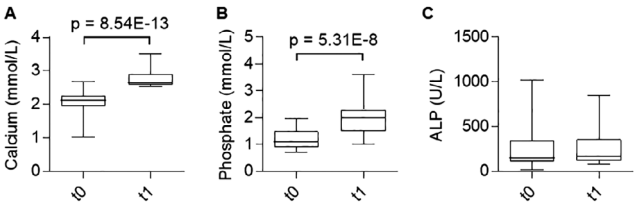

Fig 2 Bone metabolism recovery after HSCT. (*A*) Serum calcium is significantly increased after HSCT compared with the day of the HSCT. (*B*) Serum phosphate is significantly increased after HSCT compared with the day of the HSCT. (*C*) No significant difference was found between alkaline phosphatase (ALP) measurement on the day of the HSCT and the day of the patient's peak calcium.

Skeletal densitometry

ImageJ 1.47a (US National Institutes of Health, Bethesda, MD, USA)[22] was used to analyze the cortex-to-medullary density ratio. All available radiographs in the patient group of the femoral shaft region amounted to 36 radiographs of 25 patients in the early group, and 47 radiographs of 29 patients in the late group. In addition to ARO patients' radiographs, 46 radiographs of 46 patients in the control group were analyzed for comparison. Standardized regions of interest (10 by 30 pixels) were used to measure the density of the cortex (eg, Fig. 3*B–D*, {FIG3} denoted by a yellow square) and medulla (eg, Fig. 3*B–D*, denoted by a red square) at the femoral midshaft. Then, the cortical density was divided by the medullary density and multiplied by 100. To study the change in the cortex-to-medullary density ratio over time, each measurement was plotted against the time it was taken, relative to each patient's bone marrow transplant in days. A single X-ray was analyzed for the patients who had not yet undergone HSCT at the time of the data analysis. This X-ray was assigned an X value of 0 to be included in Fig. 3*E* and was included in the early group for subsequent analysis. Finally, cortex-to-medullary density ratios were statistically compared using ANOVA with Bonferroni correction for multiple comparisons between early, late, and control groups (Fig. 3*F*). Furthermore, the cortex-to-medullary density ratios were compared between the different age groups within the control group to exclude aging as a confounder of differences between the early and late groups using ANOVA with Bonferroni correction (Fig. 3*A*). A single X-ray per patient was used for each child in the following age groups: 0–3 yo (years old), 4–7 yo, 8–11 yo, and 12–15 yo.

Skeletal morphological analysis

ImageJ 1.47a was also used to analyze femoral width distribution. There were 25 full-length femur radiographs of 21 patients in the early group and 36 radiographs of 23 patients in the late group. In addition, 36 radiographs of patients in the control group were analyzed for comparison. Each radiograph was first rotated to a neutral position so the vertical axis is parallel to the length of the image. The images were cropped to include

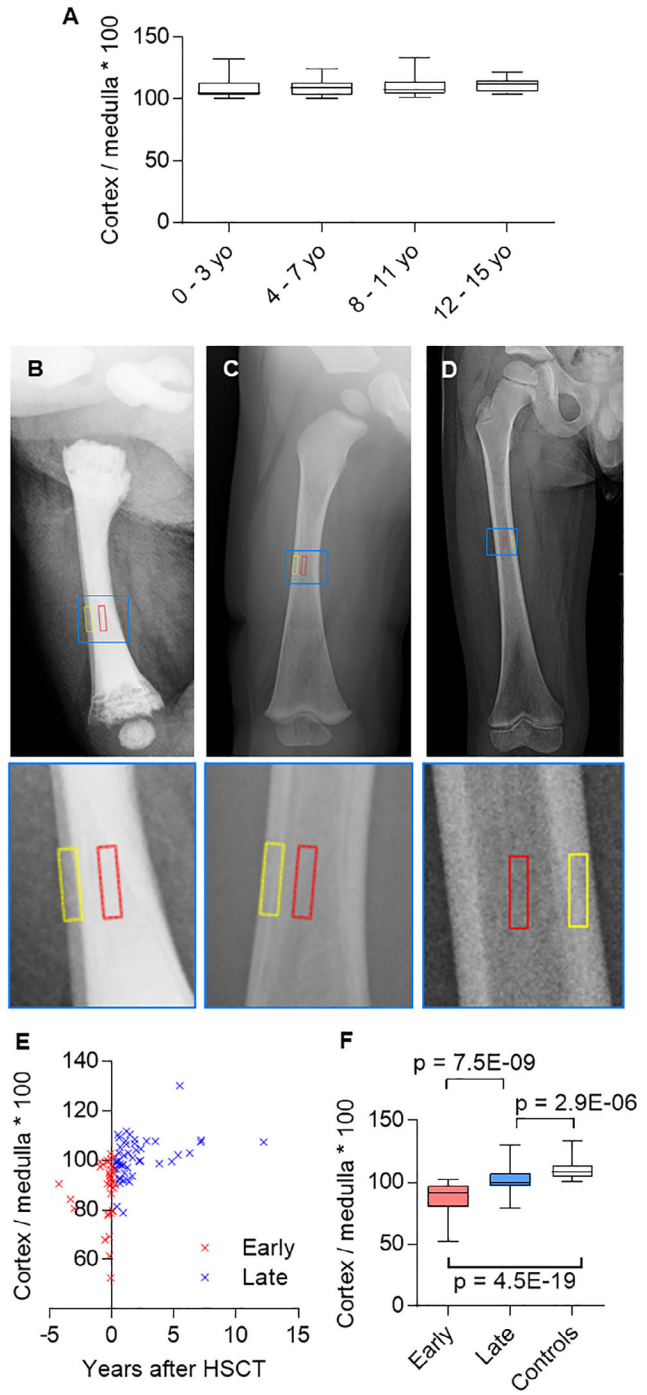

Fig 3 Skeletal mineral distribution changes after HSCT. (*A*) No significant differences in femoral cortex to medulla density ratios were found between different age groups within the controls. (*B–D*) Follow-up radiographs of a single ARO patient starting 3 months before his HSCT (*A*), to 14 months after the HSCT (*B*), and finally 5 1/2 years after the HSCT are shown (*C*). Significant changes in cortical (yellow square) and medullary (red square) mineralization are shown in the femoral midshaft (blue square, enlarged below). (*E*) Calculated cortex to medulla density ratio changes over time after the HSCT. (*F*) Significant differences in cortex to medulla density ratios between the early, late, and control groups were found.

only the metaphyses and shaft. Then, the width of the femur was measured at 10 equidistant lines along the length of the cropped image named 1 to 10 from distal to proximal, respectively (Fig. 4*A–C*). {FIG4} For each radiograph, the width measurements were normalized to the length of the image to allow comparison of growing patients. These normalized width vectors were statistically compared using ANOVA with Bonferroni correction between early, late, and control groups (Fig. 5). Furthermore, cortex-to-medullary density ratios were compared between different age groups within the control group to exclude aging as a confounder of differences between the early and late groups (Fig. 6*B*). A single radiograph per patient was used for each child in the following age groups: 0–3 yo, 4–7 yo, 8–11 yo, and 12–15 yo. Finally, the standard deviation of each normalized width distribution was calculated and compared between early, late, and control groups using ANOVA with Bonferroni correction (Fig. 6*A*).

Statistical methods

GraphPad Prism 5.0f software (GraphPad Prism, San Diego, CA, USA) was used to analyze the data. When box and whiskers are shown, whiskers represent the full range of values, the box extends from the 25th to 75th percentiles, and the line in the box is the median. To assess significance, $p < 0.05$ was considered statistically significant.

Data availability

The data sets generated and analyzed during the current study are not publicly available because of the need to protect research participants' privacy but are available from the corresponding author upon reasonable request.

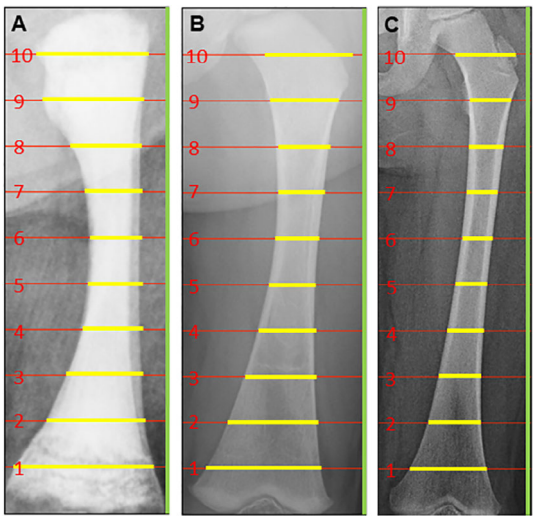

Fig 4 Qualitative skeletal morphometry changes after HSCT. (*A–C*) Follow-up radiographs of a single ARO patient starting 3 months before his HSCT (*A*), to 14 months after the HSCT (*B*), and finally 5 1/2 years after the HSCT are shown (*C*). Along the length of the femur (marked in green), 10 equidistant lines (denoted in red) are numbered 1 through 10 in each radiograph. Over these lines, the femur width distribution (highlighted in yellow) can be seen changing over time.

Results

Patient and transplant characteristics

Patient, disease, and transplant characteristics are shown in Table 1. Thirty-five patients, including 25 males and 10 females, diagnosed with OP were included in this retrospective study. Almost half of the patients were from consanguineous families. A genetic diagnosis was available for most patients. Although five different affected genes were identified in the cohort, the most common by far was TCIRG1, accounting for more than half of the identified mutations. Other patients harbored mutations in SNX10 (n = 6), CLCN7 (n = 3), OSTM1 (n = 1), and RANK (n = 3).

All patients underwent at least one HSCT, except 2 patients for whom HSCT was contraindicated based on their neurological status. Three patients underwent a second HSCT because of engraftment failure. The median age at the time of HSCT was 1.1 years and most patients were transplanted from HLA-matched donors (24/36). Matched donors included siblings (n = 13), relatives (n = 5), and unrelated donors (n = 6). Remaining patients for whom a matched donor was not available were transplanted with either a 9/10 matched family donor (n = 7) or a 9/10 matched unrelated donor (n = 3). The conditioning regimens were fludarabine-based in all cases. Half of the patients were conditioned using a combination of fludarabine, treosulfan, and thiotepa, whereas the rest were conditioned using a combination of fludarabine and busulfan with or without thiotepa or melphalan. GVHD prophylaxis in the form of either cyclosporine A alone (n = 27) or in combination with mycophenolate mofetil (n = 9) was given in all cases. Finally, most patients received in vivo T-cell depletion using anti-thymocyte globulin in all cases but one where Campath-1H was used.

Hematopoietic and bone metabolism recovery after HSCT

Hematopoietic recovery after HSCT was evaluated by studying the number of days it took patients to achieve stable non-neutropenic and non-thrombocytopenic counts (Fig. 1). The median time to stable neutrophil engraftment was 28 days (Fig. 1*A*). Similarly, the median time to stable platelet engraftment was 31 days (Fig. 1*B*).

Bone metabolism recovery was evaluated as the number of days between HSCT (t0) and peak serum calcium (t1). The median t1 was 32 days (data not shown) coinciding with hematopoietic recovery (Fig. 1). Both serum calcium (Fig. 2*A*) and serum phosphate (Fig. 2*B*) significantly increased (p = 8.54E-13 and p = 5.31E-8, respectively) between t0 and t1. Serum calcium increased from 2.2 mmol/L to 2.8 mmol/L and serum phosphate increased from 1.2 to 2 mmol/L. Serum alkaline phosphatase (Fig. 2*C*), on the other hand, was not significantly different between t0 and t1 (p = 0.068).

Skeletal mineral distribution changes after HSCT

No significant differences in cortex-to-medullary density ratios were found between different age groups in the control group of radiographs (Fig. 3*A*, p = 0.81). On the other hand, HSCT had a dramatic effect on skeletal mineral distribution (Fig. 3*B–D*). Before HSCT, femurs were overall sclerotic with increased medullary density and transverse lucent metaphyseal bands (Fig. 3*B*). After the HSCT, femurs were much less sclerotic overall and the medullary cavity was visibly less radiodense than the cortex, suggesting significant remodeling and bone mineral redistribution (Fig. 3*C*, *D*). Furthermore, the transverse lucent metaphyseal bands that were prominent before HSCT were no longer notable on late radiographs (Fig. 3*D*).

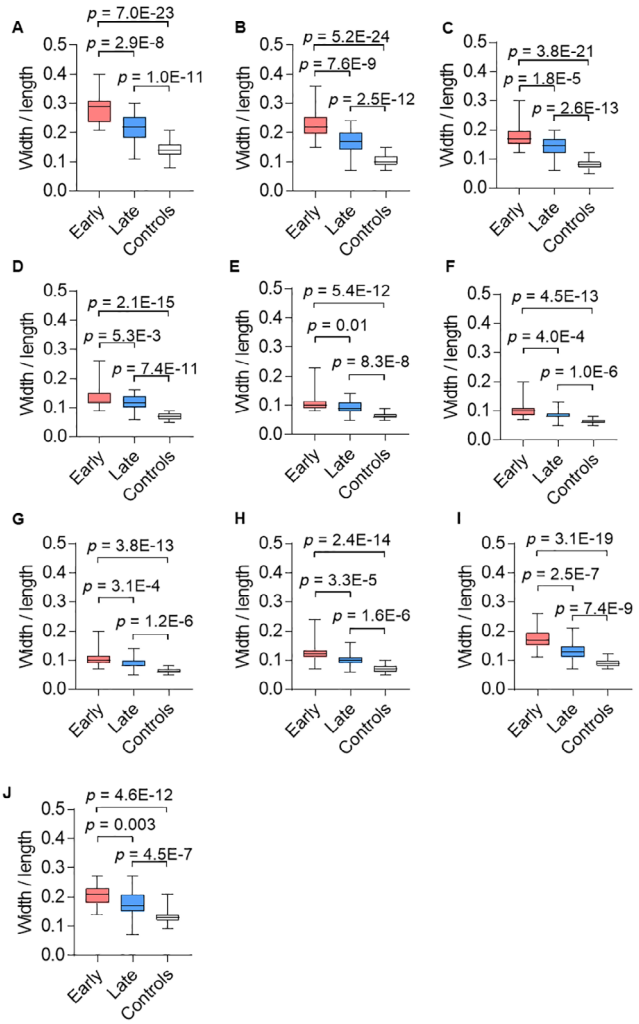

Fig 5 Quantitative femoral width changes after HSCT. Normalized femoral width was compared between the early, late, and control groups. (*A–J*) Significant differences in normalized femur widths between the study groups are shown in all 10 cross sections (1 to 10, respectively).

When the cortex-to-medullary density ratios were plotted over time with respect to the HSCT, a clear upward trend was found (Fig. 3*E*). Before HSCT, medullae were at least as radiodense as the cortices, as can be found by a cortex-to-medullary density ratio of less than a 100 in most analyzed radiographs. The late radiographs, on the other hand, taken at least 3 months after HSCT, mostly demonstrated cortex-to-medullary density ratios of more than 100. When we compared the cortex-to-medullary density ratio distributions between early (average = 89), late (average = 101), and control (average = 110) groups of radiographs, we found significant differences in all comparisons (Fig. 3*F*, p = 8.88E-18). This indicated that a significant change in mineral distribution between cortices and medullae occurred after HSCT but was not sufficient to achieve a fully normalized radiological appearance. The difference between the early and late groups cannot be attributed to the older age of the children in the late group of radiographs because mineral distribution was independent of age (Fig. 3*A*).

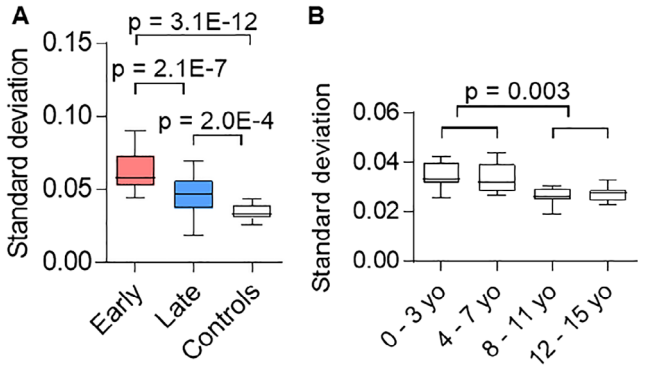

Fig 6 Femoral width distribution changes after HSCT. (*A*) Normalized femoral width distributions were found to be different between controls younger than 8 years and controls older than 8 years. (*B*) Significant differences in normalized femur width distribution standard deviations between the early, late, and control groups of radiographs are shown.

Skeletal morphological changes after HSCT

Not only skeletal mineral density but also long bone morphology was strikingly changed after HSCT. Before HSCT, Erlenmeyer flask deformities could be clearly observed, especially in the distal femoral metaphysis (Fig. 4*A*), whereas later radiographs (Fig. 4*B*, *C*) showed a gradual widening of the diaphysis and a narrowing of the metaphysis, transforming the Erlenmeyer flask deformity into a more normal morphology.

When normalized femoral width distributions were compared between the early and late groups, significant differences were found in all 10 width measurement subgroups, suggesting morphological remodeling after HSCT (Fig. 5). {FIG5} Significant differences between the late and control groups were also found in all width measurement subgroups, indicating that femoral morphology was not completely normalized. This was also evident by the significant differences in the width distribution standard deviations between all three groups (p = 8.98E-12, Fig. 6*A*). {FIG6}

The standard deviations of normalized femur widths of non-OP children older than 8 years were found to be significantly smaller than younger non-OP children (Fig. 6*B*, p = 0.003). An average reduction of 0.007 in normalized femoral width standard deviation was found in children older than 8 years compared with the younger age groups (Fig. 6*B*), suggesting that growth itself could account partially for the differences found between the early and late groups. However, since the average difference in standard deviations between the early and late groups and the late and control groups were about double (0.016 and 0.017, respectively), the difference between the controls younger than and older than 8 years, it is likely that HSCT accounts for some of the difference between early and late radiographs.

Discussion

HSCT for OP has dramatically improved patients' survival and quality of life.[14,15] Previous publications characterized the genetics and long-term outcomes of HSCT in terms of survival and HSCT-related complications. To the best of our knowledge, this is the first study to address the skeletal changes after HSCT. In this retrospective cohort, biochemical bone metabolism markers and radiographic measurements of 35 patients over 15 years of follow-up were quantitatively analyzed. This heterogeneous cohort was composed of both males and females diagnosed with five different gene mutations, treated with HSCT from related and unrelated donors (Table 1). The patients were prepared for HSCT using four different conditioning regimens, based on previously published findings,[15] and most received GVHD prophylaxis and in vivo T-cell depletion as per standard of care.

All available hematological, biochemical, and radiographic data from all patients were analyzed without any subgroup analysis to focus on the effect of HSCT on bone remodeling in skeletally immature patients with impaired osteoclast function. This is the first study to show that hematopoietic recovery after HSCT in ARO (Fig. 1) coincides with a peak in bone remodeling, evident by significant changes in serum calcium and phosphate levels (Fig. 2). These electrolyte measurements are widely available and already advocated for baseline and monitoring studies.[13]

We suggest that serum calcium and phosphate levels could be used as auxiliary indicators of engraftment in addition to neutrophil counts, platelet counts, and donor chimerism. Although complete blood counts are readily available, they are also difficult to interpret in determining stable engraftment achievement, as they are confounded by blood product transfusions, which are very common after HSCT.[23] Far less available and more expensive than complete blood counts and serum calcium and phosphate analysis is donor chimerism analysis, but it is probably the most accurate measure of engraftment available. In all, serum calcium and phosphate could be used in addition to neutrophil and platelet counts to provide a widely available and cost-effective measure of engraftment.

Unlike serum calcium and phosphate levels, the third biochemical bone metabolism marker assessed in this study, ALP, does not appear to be useful in indicating increased bone remodeling after HSCT in OP patients. Although serum calcium and phosphate levels indicated increased bone remodeling at t1, the serum ALP measurements were not significantly increased at t1. There are several possible explanations for the lack of a significant difference in serum ALP between t0 and t1 (Fig. 2*C*). Eleven of 28 patients were found to have ALP levels above the upper limit of normal at t0. Increased ALP at t0 could be secondary to an increase in the hepatic isoenzyme of ALP as a result of infection,[24] hepatotoxic medications, or both. Hepatotoxic medications including allopurinol[25] and trimethoprim-sulfamethoxazole[26] were given to all patients in the cohort, and methylprednisolone[27] was administered as indicated for GVHD. Because total serum ALP was measured in this study, rather than the bone-specific isoenzyme levels, increases in the hepatic isoenzyme could have increased the total serum ALP, thereby confounding HSCT-related changes in ALP. Future studies could use more specific bone turnover markers[28] such as bone-specific ALP, osteocalcin, and collagen type I-related peptides to examine HSCT-related changes in OP patients.

Bone remodeling was directly evaluated by quantifying both skeletal mineral distribution and morphology based on femur radiographs. These novel outcomes were found to dramatically change after HSCT. Interestingly, as early as 90 days after HSCT, a significant change was found in both bone mineral distribution and morphology (Figs. 3–6). These rapid changes cannot be the result of growth alone and are most likely attributable to recovered osteoclasts' function after HSCT. Presumably, the continued osteoclast activity throughout the follow-up period is

responsible for maintaining the improvement in mineral distribution and bone morphology noted earlier.

This is the first study to show that neither mineral distribution nor bone morphology were completely rescued after HSCT. This could be the result of insufficient follow-up length, pathological bone modeling that could not be rescued by remodeling, or suboptimal HSCT. Future studies could assess skeletal outcomes of HSCT in OP patients for longer periods of time as well as whether HSCT could be improved in order to cure the OP-associated skeletal abnormalities. Previous publications concluded that the post-HSCT morphology was completely normal by basing their observations on qualitative radiological evaluation of small cohorts and case reports.[18–20,29] The lack of a complete rescue of the skeletal phenotype should be especially valuable for orthopedic surgeons who may need to perform procedures on patients with OP after HSCT. They should consider that these patients are significantly different from non-OP patients of the same age. It is important to note that this study analyzed only femur remodeling and did not account for known radiographic differences between different forms of OP.[9] Additional limitations of this study included the limited availability of follow-up data including radiographs.

Disclosures

All authors state that they have no conflicts of interest.

Acknowledgments

The authors have no funding or industrial affiliation to declare.

Authors' roles: PS and RL designed the study and the concept. PS supervised the diagnosis, transplantation, and post-transplantation follow-up of patients. RL performed the orthopedic follow-up. NS, VG, and RL collected the epidemiological data. JF collected hematological and biochemical data. GS analyzed and interpreted the data and wrote the manuscript. All authors reviewed the draft manuscript and approved the final version for submission.

Peer Review

The peer review history for this article is available at https://publons.com/publon/10.1002/jbmr.4037.

References

1. Tolar J, Teitelbaum SL, Orchard PJ. Osteopetrosis. N Engl J Med. 2004; 351(27):2839–49.
2. Villa A, Guerrini MM, Cassani B, Pangrazio A, Sobacchi C. Infantile malignant, autosomal recessive osteopetrosis: the rich and the poor. Calcif Tissue Int. 2009;84(1):1–12.
3. Sobacchi C, Schulz A, Coxon FP, Villa A, Helfrich MH. Osteopetrosis: genetics, treatment and new insights into osteoclast function. Nat Rev Endocrinol. 2013;9(9):522–36.
4. Gerritsen EJA, Vossen JM, Vanloo IHG, et al. Autosomal recessive osteopetrosis—variability of findings at diagnosis and during the natural course. Pediatrics. 1994;93(2):247–53.
5. Dlouhy BJ, Menezes AH. Osteopetrosis with Chiari I malformation: presentation and surgical management. J Neurosurg Pediatr. 2011; 7(4):369–74.
6. Steward CG. Neurological aspects of osteopetrosis. Neuropathol Appl Neurobiol. 2003;29(2):87–97.
7. Landa J, Margolis N, Di Cesare P. Orthopaedic management of the patient with osteopetrosis. J Am Acad Orthop Sur. 2007;15(11): 654–62.
8. Ihde LL, Forrester DM, Gottsegen CJ, et al. Sclerosing bone dysplasias: review and differentiation from other causes of osteosclerosis. Radiographics. 2011;31(7):1865–82.
9. Simanovsky N, Rozovsky K, Hiller N, Weintraub M, Stepensky P. Extending the spectrum of radiological findings in patients with severe osteopetrosis and different genetic backgrounds. Pediatr Blood Cancer. 2016;63(7):1222–6.
10. Gonen KA, Yazici Z, Gokalp G, Ucar AK. Infantile osteopetrosis with superimposed rickets. Pediatr Radiol. 2013;43(2):189–95.
11. Schinke T, Schilling AF, Baranowsky A, et al. Impaired gastric acidification negatively affects calcium homeostasis and bone mass. Nat Med. 2009;15(6):674–81.
12. Stark Z, Savarirayan R. Osteopetrosis. Orphanet J Rare Dis. 2009;4 (1):5.
13. Wu CC, Econs MJ, DiMeglio LA, et al. Diagnosis and management of osteopetrosis: consensus guidelines from the osteopetrosis working group. J Clin Endocrinol Metab. 2017;102(9):3111–23.
14. Orchard PJ, Fasth AL, Le Rademacher J, et al. Hematopoietic stem cell transplantation for infantile osteopetrosis. Blood. 2015;126(2):270–6.
15. Natsheh J, Drozdinsky G, Simanovsky N, et al. Improved outcomes of hematopoietic stem cell transplantation in patients with infantile malignant osteopetrosis using fludarabine-based conditioning. Pediatr Blood Cancer. 2016;63(3):535–40.
16. Martinez C, Polgreen L, Defor T, et al. Characterization and management of hypercalcemia following transplantation for osteopetrosis. Bone Marrow Transplant. 2010;45(5):939–44.
17. Shroff R, Beringer O, Rao K, Hofbauer L, Schulz A. Denosumab for post-transplantation hypercalcemia in osteopetrosis. N Engl J Med. 2012;367(18):1766–7.
18. Cheow HK, Steward CG, Grier DJ. Imaging of malignant infantile osteopetrosis before and after bone marrow transplantation. Pediatr Radiol. 2001;31(12):869–75.
19. Costelloe CM, Eftekhari F, Petropoulos D. Radiography of successful bone marrow transplantation for osteopetrosis. Skeletal Radiol. 2007;36(Suppl 1):S34–7.
20. Hashemi Taheri AP, Radmard AR, Kooraki S, et al. Radiologic resolution of malignant infantile osteopetrosis skeletal changes following hematopoietic stem cell transplantation. Pediatr Blood Cancer. 2015;62(9):1645–9.
21. Glucksberg H, Storb R, Fefer A, et al. Clinical manifestations of graft-versus-host disease in human recipients of marrow from HL-A-matched sibling donors. Transplantation. 1974;18(4):295–304.
22. Schneider CA, Rasband WS, Eliceiri KW. NIH image to ImageJ: 25 years of image analysis. Nat Methods. 2012;9(7):671–5.
23. Shadur B, Zaidman I, NaserEddin A, et al. Successful hematopoietic stem cell transplantation for osteopetrosis using reduced intensity conditioning. Pediatr Blood Cancer. 2018;65(6):e27010.
24. Friedman LS. Approach to the patient with abnormal liver biochemical and function tests. In Chopra S, ed ; Last updated March 4, 2020. UpToDate [Internet].
25. FDA. Product information ZYLOPRIM ® (allopurinol).
26. Faria L, Resende C, Couto C, Couto O, Fonseca L, Ferrari T. Severe and prolonged cholestasis caused by trimethoprim-sulfamethoxazole: a CASE report. Clin Lett. 2009;64(1):71–4.
27. FDA. Medrol ® methylprednisolone.
28. Greenblatt M, Tsai J, Wein M. Bone turnover markers in the diagnosis and monitoring of metabolic bone disease. Clin Chem. 2017;63(2): 464–74.
29. Nour M, Ward LM. Infantile malignant osteopetrosis. J Pediatr. 2013; 163(4):1230–e1.